Magnetization Transfer Helps Detect Intestinal Fibrosis in an Animal Model of Crohn Disease[1]

Jeremy Adler, MD, MSc
Scott D. Swanson, PhD
Phyllissa Schmiedlin-Ren, MD
Peter D. R. Higgins, MD, PhD, MSc
Christopher P. Golembeski, MD
Alexandros D. Polydorides, MD, PhD
Barbara J. McKenna, MD
Hero K. Hussain, MD
Trevor M. Verrot, BA
Ellen M. Zimmermann, MD

Purpose: To determine the utility of magnetization transfer (MT) in the identification and quantification of intestinal fibrosis in a rat model of Crohn disease.

Materials and Methods: The university committee on the use and care of animals approved this study (UCUCA 08592). Lewis rats injected subserosally with peptidoglycan-polysaccharide (PG-PS) develop bowel inflammation 1 day after laparotomy (early phase) and fibrosis starting 14 days after laparotomy (late phase). The authors performed 2.0-T magnetic resonance (MR) imaging in 25 rats injected with PG-PS and 13 injected with human serum albumin (HSA) (control animals). Imaging was performed before laparotomy and on a weekly basis thereafter for up to 28 days. The MT ratio in the bowel wall was calculated. Resected cecal tissue was scored for inflammation and fibrosis. Tissue fibrosis was determined with colorimetric analysis of trichrome-stained specimens. Collagen content was measured with Western blot analysis. Statistical analyses were performed with the Student *t* test for continuous bivariate comparisons, the Pearson correlation for continuous variables, and the Spearman correlation for ordinal variables.

Results: All rats developed early inflammation, which subsided over time. Rats injected with PG-PS developed increased fibrosis in the late phase, whereas control rats did not. The mean MT ratio of rats injected with PG-PS with late-phase fibrosis was higher than that in rats with early phase inflammation ($P = .017$). In addition, the MT ratio of rats injected with PG-PS with late-phase fibrosis was higher than that of control animals that did not develop fibrosis in the late phase ($P = .0001$). The MT ratio of control animals remained unchanged over time as inflammation subsided. The MT ratio in rats injected with PG-PS showed correlation with tissue fibrosis ($\rho = 0.63$). The MT ratio showed correlation with tissue collagen ($R = 0.74$). The positive and negative predictive values of the MT ratio in the prediction of fibrosis were 92% (12 of 13 rats) and 83% (five of six rats), respectively.

Conclusion: These results indicate that MT is sensitive to bowel wall fibrosis as occurs in Crohn strictures.

Supplemental material: *http://radiology.rsna.org/lookup/suppl/doi:10.1148/radiol.10091648/-/DC1*

[1] From the Department of Pediatrics, Division of Gastroenterology, University of Michigan Medical Center, 1150 W Medical Center Dr, A520B MSRB I, Box 5658, Ann Arbor, MI 48109. Received October 7, 2009; revision requested November 24; revision received August 18, 2010; accepted September 4; final version accepted September 20. Supported by the University of Michigan Gut Peptide Research Center. **Address correspondence to** J.A. (e-mail: *jeradler@umich.edu*).

The natural history of Crohn disease involves chronic, transmural bowel wall inflammation that often leads to luminal narrowing and results in intestinal strictures or bowel obstruction. Intestinal strictures promote the formation of fistulas (1,2). Histologically, Crohn strictures typically contain a mixture of inflammatory and mesenchymal cells along with extracellular matrix components with varying degrees of fibrosis. Clinically, strictures can behave as predominantly inflammatory or fibrotic in nature, which creates both diagnostic and therapeutic dilemmas. An intestinal stricture that is largely inflammatory often responds quickly to high-dose steroid therapy or therapy with potent anti–tumor necrosis factor α agents. This may relieve the intestinal obstruction but exposes the patient to the numerous potential side effects of medical therapy, including the deleterious effects of steroids on the growth and development of children (3–7). An intestinal stricture that is primarily fibrotic in nature will not respond to current medical treatment; however, it requires surgical resection (8). To our knowledge, there are currently no clinical findings, laboratory measurements, or imaging modalities that allow the clinician to specifically determine the degree of fibrosis present in an intestinal stricture. Furthermore, efforts at investigating treatment modalities to prevent or treat intestinal fibrosis are hampered by the lack of a useful test for fibrosis to study the natural history of Crohn disease.

We investigated magnetization transfer (MT) magnetic resonance (MR) imaging to specifically address the need for a noninvasive test to quantitate intestinal fibrosis. MT MR imaging depicts different molecular properties than does conventional MR imaging. Whereas the contrast between different tissues in MR is a complicated function of tissue properties and pulse sequence parameters, MT generates contrast that is primarily determined by the fraction of large macromolecules or immobilized phospholipid cell membranes in tissue (9,10). Because of this increased specificity, MT should be more sensitive to the changes in collagen content that occur in fibrotic bowel tissue with strictures and, thus, enable the differentiation of those tissues from bowel tissues that contain less collagen (eg, edematous or inflamed tissues).

The purpose of this study was to determine the utility of MT in the identification and quantification of intestinal fibrosis in a rat model of Crohn disease. We hypothesized that MT would help differentiate fibrotic from nonfibrotic tissue and that the MT ratio would correlate with intestinal collagen content in an animal model of Crohn disease. To investigate this approach, we studied a well-characterized rat model of Crohn disease typified by an early phase of intestinal inflammation and a late phase of intestinal fibrosis.

Advances in Knowledge

- We have demonstrated that magnetization transfer (MT) MR imaging depicts bowel wall fibrosis in an animal model of Crohn disease.
- The MT ratio helps differentiate fibrosis from inflammation in vivo; the mean MT ratio (±standard deviation) in the fibrotic bowel was 33.4 ± 11.8, and the mean MT ratio in the inflamed bowel was 15.7 ± 2.1 (P = .02).

Implications for Patient Care

- The ability to detect fibrosis in small bowel Crohn strictures may help the clinician make decisions regarding medical therapies for nonfibrotic bowel and surgical interventions for fibrotic strictures.
- The ability to identify and grade the degree of fibrosis and monitor changes in fibrosis may assist in the evaluation of new therapeutic agents targeted at treating fibrotic strictures, which currently cannot be studied owing to the lack of a noninvasive means for monitoring changes in fibrosis.

Materials and Methods

Animal Model

All animal studies were approved by the University of Michigan Committee on the Use and Care of Animals (UCUCA 08592). Thirty-eight specific pathogen-free adult female Lewis rats were obtained from Harlan (Indianapolis, Ind). The animals were housed under standard specific pathogen-free conditions and had free access to water and standard laboratory chow.

During laparotomy, purified peptidoglycan-polysaccharide (PG-PS) was injected intramurally (12.5-μg rhamnose per gram of body weight, 0.05 mL per injection site) into standardized locations in the cecum, distal ileum, and Peyer patches of 25 rats (11). Thirteen control animals were similarly injected with human serum albumin (HSA). In the early phase after injection, rats injected with PG-PS develop inflammation, with tissue edema at the injection sites in the first 24 hours. The late phase, which begins approximately 14 days after laparotomy, is typified by inflammation and intense fibrosis (11). Within 21 days after laparotomy, rats develop bowel wall thickening and intraabdominal adhesions. In addition, the bowel, liver, and spleen are studded with granulomas. Control animals injected with

Published online before print
10.1148/radiol.10091648

Radiology 2011; 259:127–135

Abbreviations:
HSA = human serum albumin
MT = magnetization transfer
PG-PS = peptidoglycan-polysaccharide
RF = radiofrequency
ROI = region of interest

Author contributions:
Guarantor of integrity of entire study, E.M.Z.; study concepts/study design or data acquisition or data analysis/interpretation, all authors; manuscript drafting or manuscript revision for important intellectual content, all authors; manuscript final version approval, all authors; literature research, J.A., S.D.S., P.D.R.H., E.M.Z.; experimental studies, J.A., S.D.S., P.S.R., B.J.M., T.M.V., E.M.Z.; statistical analysis, J.A., P.D.R.H.; and manuscript editing, J.A., S.D.S., P.S.R., P.D.R.H., A.D.P., B.J.M., H.K.H., E.M.Z.

Funding:
This research was supported by the National Institutes of Health (grants NIDDK R01 DK073992, NICHD K12 HD028820, and NIH NIDDK P30 DK 34933-22).

Authors stated no financial relationship to disclose.

See also Science to Practice in this issue.

HSA do not develop late-phase inflammation or fibrosis (Fig 1).

Imaging Protocol

All MR images were obtained with a 2.0-T, 31-cm clear-bore system equipped with actively shielded gradients (Inova; Unity Varian, Palo Alto, Calif). Resected intestinal tissue from two rats—one control rat and one rat injected with PG-PS with late-phase fibrotic enterocolitis—was imaged ex vivo in nonimaging nuclear MR spectroscopy mode. MT z-spectra were obtained with 25 off-resonance frequencies (logarithmically from 100 Hz to 100 kHz) and four radiofrequency (RF) power levels (2.82, 5.64, 11.28, and 22.55 μT) (12). The results of these studies were used to select the off-resonance frequency and RF power to generate significant MT and minimize direct RF saturation (13).

For in vivo imaging, a multisection gradient-echo pulse sequence (repetition time msec/echo time msec = 400/3.5) was used to generate MT with a 20-msec sinc pulse applied 10 kHz off-resonance. The 20-msec MT pulse had an effective continuous wave RF power of 312 Hz (7.33 μT) (14). Other imaging parameters were as follows: 2-mm-thick sections, 0.47-mm in-plane resolution, and 30° excitation pulse. For in vivo studies, a few rats from each experiment were sedated with isoflurane and underwent baseline MT MR imaging 1 day before laparotomy and injection of PG-PS or HSA, as described earlier. MT MR imaging was performed in a standard imaging mode at 10 kHz to generate images with optimal MT (M_{sat} images) and at 100 kHz off-resonance to generate images without MT (M_0 images). The MT ratio in the cecal wall was calculated as follows: 100(1 − MT on M_{sat} image/MT on M_0 image). Representative conventional and MT images in normal rats are shown in Figure 2.

Four in vivo experiments were performed (Table 1). The first two experiments (experiments 1 and 2) were designed to determine whether MT could help differentiate fibrotic from nonfibrotic bowel in vivo. These rats underwent their final MT imaging examination 21 days after laparotomy. In the next experiment (experiment 3), we evaluated whether MT imaging could help assess changes in fibrosis over time. Rats underwent MR imaging on a weekly basis for 28 days after laparotomy. The fourth experiment (experiment 4) specifically addressed the question of whether MT MR imaging could help differentiate fibrosis from inflammation. Rats evaluated in the early phase underwent their final MT MR imaging examination 1 day after laparotomy, during the time of intense inflammation and minimal fibrosis. Rats evaluated in the late phase underwent weekly MT imaging examinations until their final examination, performed 21 days after laparotomy, during the time of maximal fibrosis and decreased inflammation.

On each image, regions of interest (ROIs) were identified on the greater curve of the cecum and at the cecal tip in the general vicinity of where the injections were to have been performed. ROIs were selected in areas in which the bowel wall was clearly well defined and visible on both the M_{sat} and M_0 images. Two to five ROIs were identified for each image with use of imaging software for a Macintosh computer (Osirix version 3.5.1; Osirix, Geneva, Switzerland). The ROIs varied in size and included the full thickness of the bowel wall, with a maximum length of one-fourth the circumference of the cecum in cross section. Once defined on the M_0 image, the ROI was then copied and applied to the corresponding M_{sat} image. If necessary, to account for bowel motion, minor adjustments for position were made at the time the ROI was copied without otherwise changing its size or dimensions. One author (J.A.) identified the ROIs in a blinded manner. If no suitable corresponding image was available, consensus was sought with a second reviewer (P.S.R. or S.D.S.). If no suitable ROI could be identified, then no measurement was made.

Evaluation of Gross Pathologic Specimens

After the final image was obtained, rats were sacrificed and the cecums were grossly evaluated by an observer blinded to the treatments. Evaluation was performed primarily by E.M.Z., P.S.R., and J.A., who have 20, 7, and 4 years of experience, respectively, with this method of assessment. Cecal wall thickening, mesenteric thickening, and adhesions were graded on a scale of 0 to 4 according to the degree of opacity of the bowel wall and the perceived thickness at palpation. The composite gross gut score, a well-established means of assessment of fibrosis, was calculated as the sum of the individual scores and determined for all rats upon dissection. (15–17).

Histologic Evaluation

Samples of the excised cecum were fixed in neutral buffered formalin, embedded

Figure 1

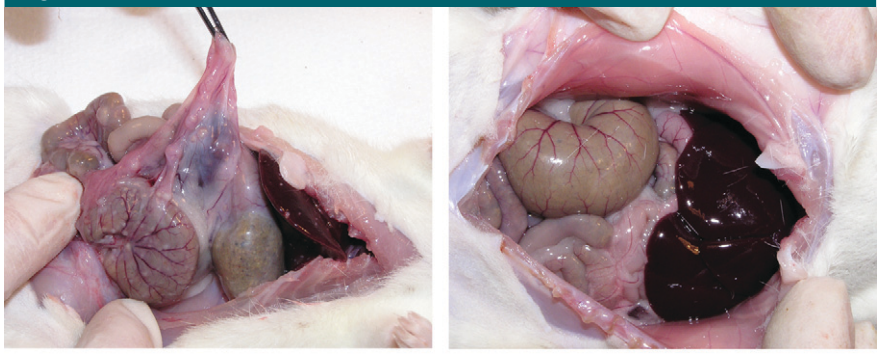

a. b.

Figure 1: **(a)** Gross dissection of rat injected with PG-PS. There are marked adhesions, and granulomas are located on the surface of the bowel and liver edge as well as throughout the mesentery. **(b)** Gross dissection of control rat injected with HSA. The bowel and liver appear normal.

Figure 2

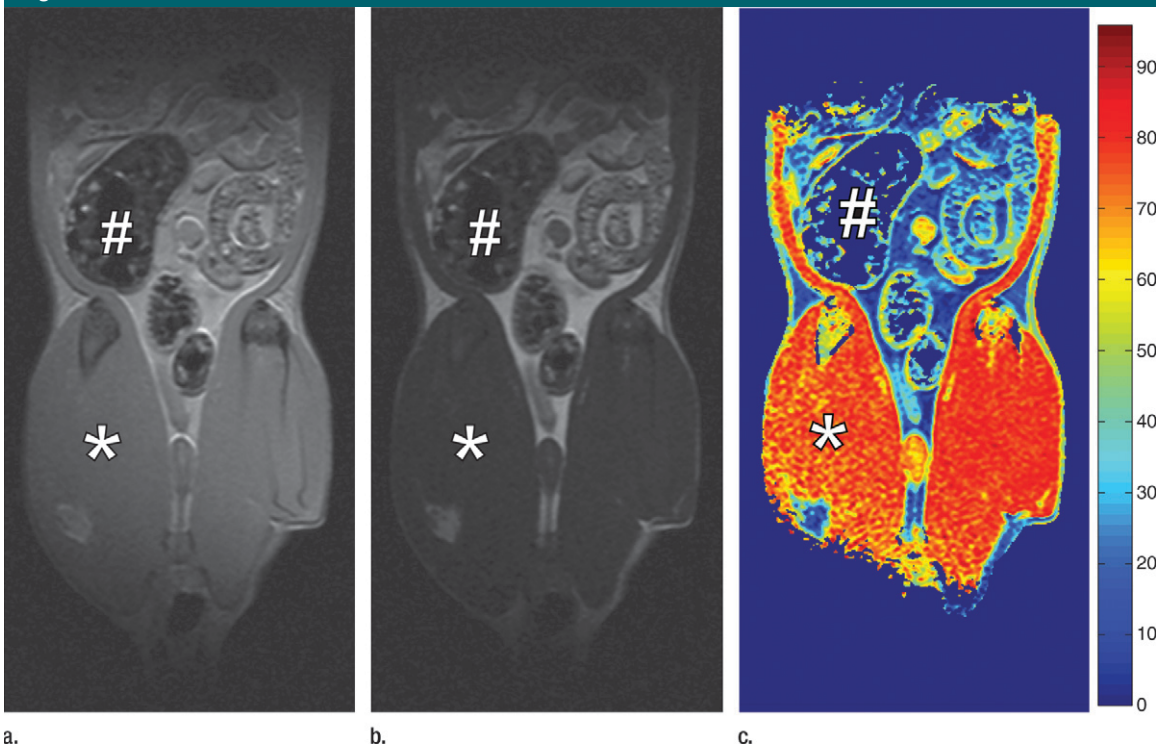

Figure 2: Coronal MR images of normal rat abdomen obtained with a spin-echo sequence (3000/20) and RF saturation pulses at **(a)** 100 kHz and **(b)** 10 kHz off-resonance. The gaussian-shaped MT saturation pulses were applied with a duration of 120 msec during the quiescent periods of the multisection imaging sequence. The RF pulse at 100 kHz off-resonance is outside of the resonance line of the immobilized molecules and does not generate any MT, whereas the RF pulse at 10 kHz generates substantial MT. **(c)** Image of the computed MT ratio. Normal bowel has a low MT effect, whereas a stiff tissue such as muscle has a high MT effect owing to the high content of myosin and other muscle macromolecules. # = cecum, * = muscle of the lower extremity.

in paraffin, and sliced. Specimens were removed from paraffin and stained with Masson trichrome. With use of an eyepiece reticle in a standard light microscope, the thickness of the cecal wall was measured by an observer (P.S.R.) blinded to the treatment group. Measurements were made in two to six regions in which full-thickness tissue was clearly identifiable, not associated with plicae, and judged to be suitably oriented. The mean thickness was calculated across all measurements. Two gastrointestinal pathologists (B.J.M. and C.P.G.) blinded to the treatment history graded the tissue in consensus with regard to the degree of inflammation and degree of fibrosis on a scale of 0 to 4 (Table 2) (18). The thickness of the resected cecal tissue was measured at microscopy in the 21 rats evaluated in experiments 1–3 (16 injected with PG-PS and five control animals, Table 1). The histologic fibrosis score was determined in the 17 rats evaluated in experiment 4 (nine injected with PG-PS and eight control animals).

Collagen Measurement

Resected cecal tissue was frozen in liquid nitrogen at the time of dissection. The frozen rat cecal tissue from 23 rats (experiments 1–3) was placed in buffer (150 mmol/L sodium chloride, 25 mmol/L Tris, 2 mmol/L edetic acid, 2 mmol/L ethylene glycol tetraacetic acid, 1 mmol/L sodium orthovanadate, 0.1% sodium dodecyl sulfate, 1% Triton X-100 [Sigma Chemical, St Louis, Mo], 0.5% sodium deoxycholate; pH, 7.4) with protease inhibitors (1 mmol/L phenylmethylsulfonyl fluoride, 0.2 TIU/mL aprotinin, 10 μg/mL leupeptin) in a hand-held conical tissue grinder with a ground-glass pestle and was homogenized. The protein concentration was measured with Bradford protein assay by using bovine serum albumin standards. With use of a denaturing but nonreducing sample buffer, samples (50 μg per lane) were electrophoresed in 8% polyacrylamide gels with 4.5% stacking gels at 150 V for 1 hour. Proteins were electrophoretically transferred to PVDF (polyvinylidene fluoride) membranes overnight at 30 V. After blocking in 5% nonfat dry milk in Tris-buffered saline with 0.3% Tween 20 (Sigma Chemical), the blots were incubated with rabbit anticollagen I (Rockland Immunochemicals, Gilbertsville, Pa; 1:1000) overnight at 4°C. After washing, the blots were incubated with horseradish peroxidase–labeled goat antirabbit immunoglobulin G (Santa Cruz Biotechnology, Santa Cruz, Calif; 1:10000) for 1 hour at room temperature. The blots were then washed, incubated with a chemiluminescence reagent (Super Signal West Dura; Pierce Biotechnology, Rockford, Ill),

and exposed to film (Hyperfilm ECL; Amersham-GE Healthcare, Piscataway, NJ). Densitometry of developed films was performed by using public domain software (Image J program, developed at the National Institutes of Health and available at *http://rsb.info.nih.gov/nih-image/*).

Colorimetric Analysis of Trichrome-stained Tissue

Tissue sections were digitally imaged (SprintScan 35 Plus, model CS-3600; Polaroid, Minnetonka, Minn) and recorded in tagged image file format. Image analysis was performed with a Macintosh computer (model OS 10.5.6). The white background on the image was removed with Adobe Photoshop CS3 (version 10.0.1; Adobe Systems, San Jose, Calif), and color segmentation analysis was performed with software (MatLab R2009a; MathWorks, Natick, Mass). Colors were then converted into HSV (hue, saturation, value) color space (19,20). Each pixel was categorized according to its color to identify its likely tissue type. Collagen area was defined as the distinct blue region and was differentiated from muscle, blood, and inflammatory cells. The total length of each cecal tissue segment was measured. In cases of curved tissue, multisegment measurements were performed along the axis of the muscularis propria, without regard to plicae. All linear measurements were performed by J.A. with use of scanned images and Osirix software. The collagen area of cecal tissue was standardized to tissue section size by dividing the blue collagen area by the tissue length of the specimen.

Statistical Analysis

For each image, we calculated the mean MT ratio across all ROIs. All results are expressed as means ± standard deviations. For all bivariate comparisons of sample means (MT ratio, collagen content with Western blot analysis, and collagen content per unit length), the two-tailed Student *t* test was used. For all correlations of continuous variables (MT ratio, collagen content with Western blot analysis, collagen content per unit length, and tissue thickness), the Pearson correlation was performed with Bonferroni adjustment for multiple comparisons as appropriate. For all ordinal comparisons (histologic fibrosis score, histologic inflammation score, and gross gut score), the Spearman correlation was performed with Bonferroni adjustment for multiple comparisons as appropriate. The diagnostic accuracy of the MT ratio for fibrosis was assessed with receiver operating characteristic curves. All statistical analyses were performed with software (Stata 10.1 for Mac; StataCorp, College Station, Tex).

Table 1

Summary of Experiments

Experiment	No. of Rats Injected with PG-PS	No. of Rats Injected with HSA	Description
Ex vivo experiment (RF findings)	1	1	Four RF power levels in ex vivo tissue
In vivo experiments			
1 (fibrotic vs nonfibrotic bowel)	6*	1	MT MR imaging at day 21
2 (fibrotic vs nonfibrotic bowel)	8	2	MT MR imaging at day 21
3 (changes in fibrosis over time)	2	2	Weekly MT MR imaging to day 28
4 (fibrosis vs inflammation and changes in fibrosis over time)	Early phase: 5; late phase: 4	Early phase: 4; late phase: 4	Early phase: MT MR imaging on day 1 to examine inflammation; late phase: weekly MT MR imaging to day 21 to evaluate fibrosis

* MT MR images in two rats were unreadable.

Table 2

Description of Histologic Scores

Score	Inflammation	Fibrosis
0	None	None
1	Focal mural or subserosal inflammation	Mild increase in collagen, focal distribution in submucosal fibrosis
2	Patchy mural or subserosal inflammation	Patchy distribution, thicker layer, no expansion of lamina propria
3	Diffuse mural inflammation	Thick layer, slight expansion of lamina propria
4	Diffuse mural and subserosal inflammation	Expansion of lamina propria involving muscularis propria

Results

MT Ratio in Fibrotic versus Nonfibrotic Bowel

Two MR images in the PG-PS group were uninterpretable and excluded from analysis. When all rats evaluated in the late phase were taken together, the MT ratio of the 18 rats injected with PG-PS (mean MT ratio, 24.7 ± 1.9) was significantly higher than that of the nine rats injected with HSA (mean MT ratio, 10.8 ± 1.7) ($P = .0001$, Fig 3). Rats injected with PG-PS developed thick fibrotic bowel, which was seen histologically as bands of collagen through the submucosa (Fig 4b) and hyperplasia of the muscularis externa. The intestines of control animals essentially appeared normal, without fibrosis (Fig 4d). The MT MR images of the rats injected with PG-PS that developed fibrotic bowel demonstrated thickened bowel wall with intense red signals, which represents a higher MT ratio on color gradient images (Fig 4a); this finding was not seen in control rats without fibrosis (Fig 4c).

Figure 3

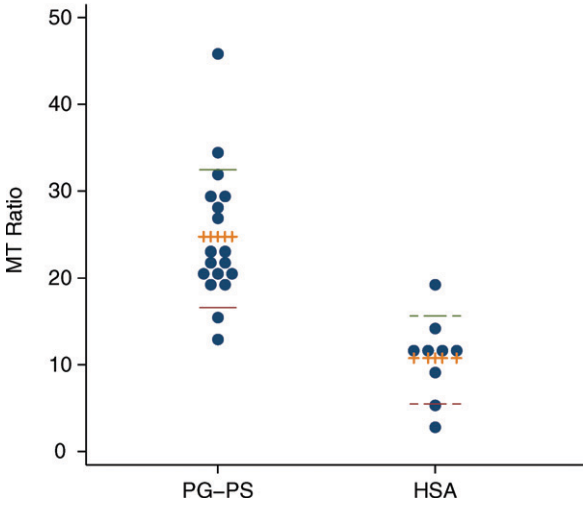

Figure 3: Dot plot of MT ratio in rats evaluated in the late phase across all experiments. Eighteen rats were injected with PG-PS (mean MT ratio, 24.7 ± 1.9) and nine with HSA (mean MT ratio, 10.8 ± 1.7) (P = .0001). Dashed and solid lines indicate the upper and lower quartiles, respectively. Hatched lines indicate mean values.

The MT ratio showed good correlation with the quantity of type I collagen (19 rats; R = 0.74, P = .0003; Fig 5). In addition, compared with control animals, rats injected with PG-PS expressed markedly increased type I collagen, as measured with Western blot analysis (19 rats; 319.4 densitometric units [DU] ± 22.4 vs 1404.6 DU ± 179.9, respectively; P = .003; Fig E1, online). The MT ratio was also shown to correlate with the gross fibrosis score (35 rats; ρ = 0.61, P = .0001; Fig E2a, online) and with tissue thickness at histologic examination (19 rats; R = 0.55, P = .015; Fig E2b, online). Tissue inflammation showed a weak correlation with MT ratio (16 rats; ρ = 0.49, P = .057; Fig E3, online).

To determine the ability of MT to help differentiate between fibrotic and nonfibrotic tissues, arbitrary cutoff values were assigned for collagen (≥500 DU at Western blot analysis, 19 rats), fibrosis (histologic fibrosis score ≥2, 16 rats), and MT ratio (MT ratio ≥15, 16 rats). Cutoff values were assigned on the basis of visual assessment of the data, with determination of these numbers as the natural break points (Tables E1 and E2, online). Given these parameters, the positive predictive value for MT ratio in the prediction of fibrosis measured with collagen Western blot analysis was 92% (12 of 13 rats) and the negative predictive value was 83% (five of six rats). The positive predictive value of the MT ratio in the prediction of fibrosis assessed with the histologic fibrosis score was 44% (four of nine rats) and the negative predictive value was 86% (six of seven rats). In the prediction of fibrosis with the MT ratio, the area under the receiver operating characteristic curve was 0.88 with use of collagen measured with Western blot analysis and 0.67 with histologic fibrosis score (Fig E4, online).

MT Ratio Parallels the Development of Fibrosis

Rats were studied with serial MT imaging to determine the sensitivity of MT to changes in fibrosis over time. Two cohorts were studied (experiment 3 and the late phase of experiment 4; see Table 1 and Table E3 [online]). The MT ratio increased in rats injected with PG-PS, which is consistent with the onset of the late fibrotic phase of PG-PS–induced enterocolitis (15). Rats injected with HSA demonstrated no significant change in MT ratio over time. The time course of all rats is shown in Figure 6.

MT Ratio in Fibrotic vs Inflamed Bowel

Experiment 4 (Table 1) addressed the ability of MT MR imaging to help differentiate inflammation from fibrosis. None of the rats demonstrated fibrosis 1 day after laparotomy (early phase) (mean histologic fibrosis score: 0.2 ± 0.2 in rats injected with PG-PS and 0.8 ± 0.3 in control rats; P = .13). Within 21 days after laparotomy (late phase), rats injected with PG-PS developed intense fibrosis whereas rats injected with HSA did not (mean histologic fibrosis score: 4.0 ± 0.0 vs 1.0 ± 0.4, respectively; P = .0003). The mean histologic fibrosis score in rats injected with PG-PS increased significantly from day 1 to day 21 (from 0.2 ± 0.2 to 4.0 ± 0.0, P < .0001) (Fig 7, center chart). This paralleled an increase in the mean MT ratio of rats injected with PG-PS from day 1 to day 21 (from 15.7 ± 2.1 to 33.4 ± 5.0, P = .02) (Fig 7, right chart). The MT ratio in rats injected with HSA did not change significantly between day 1 and day 21 (P = .69). Conversely, the inflammation score decreased during this period (Fig 7, left chart). The increase in the MT ratio concomitant with the increase in tissue fibrosis and decrease in tissue inflammation supports our hypothesis that it is sensitive to changes in fibrosis but not to changes in tissue inflammation.

Trichrome Colorimetric Analysis

To establish that the two methods of collagen measurement were in agreement, we correlated findings with the two methods: MatLab trichrome colorimetric analysis and Western blot for type I collagen. Standardized collagen area determined with MatLab trichrome colorimetric analysis showed correlation with tissue collagen determined with Western blot analysis for type I collagen (20 rats, R = 0.69, P = .0007) (Fig E5, online).

Discussion

In this study, we demonstrated that MT can help identify intestinal fibrosis in vivo in a rat model of Crohn disease. We found that the MT ratio in fibrotic segments of bowel wall in rats with PG-PS–induced intestinal fibrosis was higher than that in the nonfibrotic bowel of control animals treated with HSA.

Biomarkers and imaging modalities are extremely useful in clinical practice and in clinical trials for assessing clinical activity from Crohn disease that reflects tissue inflammation. Currently, no available tool exists that assesses tissue

Figure 4

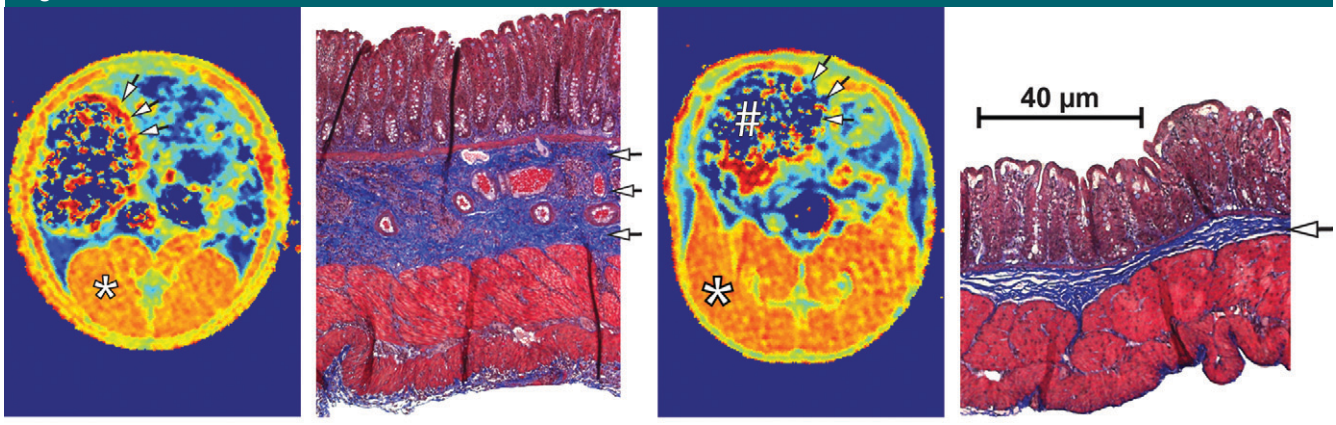

Figure 4: **(a, c)** In vivo transverse MT MR images and **(b, d)** corresponding Masson trichrome–stained slices of cecum from rats injected with PG-PS **(a, b)** or HSA **(c, d)**. Images were obtained 21 days after laparotomy. A gradient pulse sequence (400/3.5) was used to generate MT, with a 20-msec sinc pulse applied 10 kHz off-resonance. The 20-msec MT pulse had an effective continuous wave RF power of 312 Hz (7.33 μT) (14). Other imaging parameters were as follows: 2-mm-thick sections, 469-μm in-plane resolution, and 30° excitation pulse. MT images are colorized with color gradients representing the MT ratio (scale is shown in Fig 2). Note that the MT ratio in the bowel of the rat injected with PG-PS is high, which is indicated by the red color (arrows in **a**); this area corresponds to the thickened bowel wall of the same rat **(b)** with markedly expanded collagen (arrows in **b**), which is stained blue. The MT ratio in the bowel of the rat injected with HSA is low (arrows in **c**). This area corresponds to the thin bowel wall of the same rat **(d)** with a normal thin layer of collagen (arrows in **d**), which is stained blue. # = cecum, * = paraspinous muscle.

fibrosis. Because fibrosis is key to the natural history of Crohn disease, it follows that there is no test that is able to adequately monitor the natural history of Crohn disease. To our knowledge, MT MR imaging is the first noninvasive cross-sectional imaging technique that can semiquantitatively depict intestinal fibrosis.

Other imaging modalities have been investigated in an attempt to identify a technique for the noninvasive quantification of bowel wall fibrosis. Findings at computed tomography (CT) thought to be suggestive of fibrosis include bowel wall thickening in the absence of contrast enhancement (21). However, this has not been demonstrated in studies directly assessing resected intestinal tissue (22). Positron emission tomography (PET)/CT was initially thought to have great potential in the quantitation of intestinal fibrosis. However, the high concentration of leukocytes in all strictures, both fibrotic and nonfibrotic, leads to a substantial accumulation of fluorine 18 fluorodeoxyglucose, which overshadows any ability to detect collagen in strictures. This was illustrated by Jacene et al (23), who investigated PET/CT in patients known to have small bowel strictures before surgery. They found that PET/CT was sensitive to inflammation but unable to depict differences among fibrosis, muscular hypertrophy, and inflammation (23). Ultrasonography (US) is exquisitely sensitive to bowel wall changes in accessible regions of bowel, although its ability to help differentiate inflammation from fibrosis has traditionally been limited. Maconi et al (24) found that echo patterns differed between fibrotic and inflammatory strictures in ileal Crohn disease. Nylund et al (25) made similar observations. They found that the stratification of tissue layers at US is more discrete in fibrotic strictures than in tissue layers of inflammatory strictures. Although this is more specific than previous imaging studies, conventional US does not appear to be able to help

Figure 5

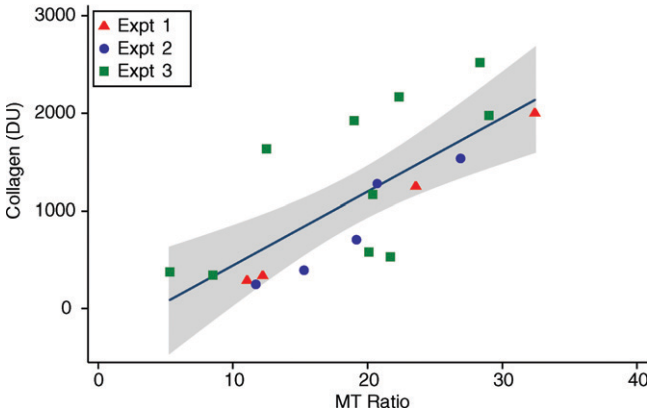

Figure 5: Graph shows the relationship between MT ratio and tissue collagen in rats injected with PG-PS and HSA (experiments 1–3). Tissue collagen was measured by means of Western blot assay and is represented in densitometric units. Pairwise correlation was calculated with the Pearson correlation coefficient (19 rats; $R = 0.74$, $P = .0003$). The shaded region represents the 95% confidence interval from linear regression of collagen on MT ratio. *Expt* = experiment.

Figure 6

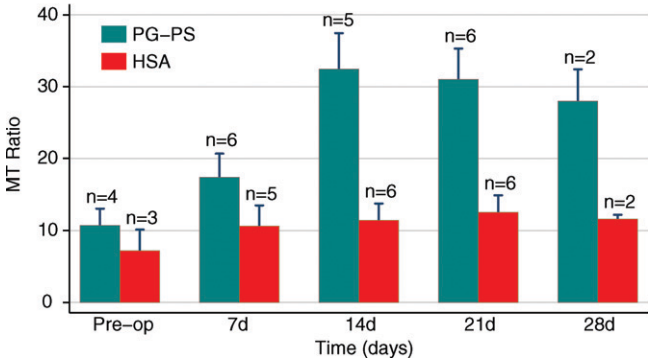

Figure 6: Bar chart shows the changes in the MT ratio over time. MT MR imaging was performed before laparotomy (*Pre-op*) and then weekly thereafter for up to 28 days. Note the progressive increase in the MT ratio in rats injected with PG-PS. This is consistent with the development of intestinal fibrosis in this model. Control animals had a lower MT ratio and did not develop fibrosis. There were no significant differences between the MT ratio in rats injected with PG-PS and that in control rats before ($P = .4$) and 7 days after ($P = .2$) laparotomy. Beginning 2 weeks after injection, the MT ratio in rats injected with PG-PS was significantly greater than that in control rats ($P = .003$). Numbers are numbers of rats.

Figure 7

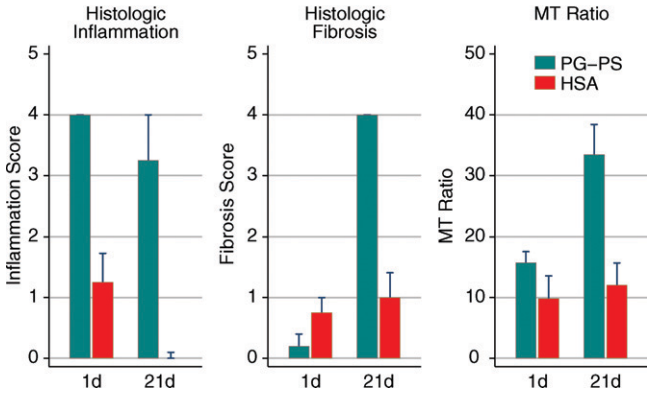

Figure 7: Bar charts show the changes in histologic inflammation, histologic fibrosis, and MT ratio from 1 day (early inflammatory phase) to 21 days (late fibrotic phase) after laparotomy. Note that the MT ratio of rats injected with PG-PS increased from day 1 to day 21, in parallel with the increase in fibrosis and opposite to the change in inflammation, which decreased somewhat. Control animals demonstrated no increase in MT ratio or fibrosis, and inflammation resolved completely.

differentiate subtle gradations in fibrosis. US elasticity imaging was recently shown to enable the quantitative measurement of bowel wall fibrosis in a rat model of Crohn disease (26). This technique seems to hold great promise. MR enterography provides detailed images of the bowel and extraintestinal structures and clinically useful information (27). Punwani et al (28) found that layered enhancement at MR enterography is associated with fibrostenotic disease. However, they also found that homogeneous enhancement had a stronger association with fibrostenotic disease. Previous studies have attempted to differentiate fibrotic from nonfibrotic signal on the basis of their signal intensities at T1- versus T2-weighted imaging or their specific pattern of enhancement with T2-weighted fast imaging employing steady-state acquisition sequences (29). To our knowledge, however, no study to date has clearly demonstrated the ability to differentiate fibrotic from nonfibrotic bowel (30).

We also demonstrated that MT imaging can depict changes in the degree of tissue fibrosis over time. Rats with PG-PS–induced enterocolitis develop a typical sequence of events with early inflammation that progresses to increasing bowel wall fibrosis beginning at approximately 1–2 weeks after injection. In these experiments, we demonstrated that the MT ratio is sensitive to these changes in bowel fibrosis that were detected in the rats treated with PG-PS but not in control animals that did not develop fibrosis. Detecting changes in fibrosis over time has clinical utility for monitoring patients with a stricturing phenotype of Crohn disease. This finding also has the potential to be of great benefit as a research tool for monitoring the natural history of Crohn disease.

We further demonstrated the ability of MT to help differentiate fibrotic from inflamed bowel in the PG-PS model. We took advantage of an interesting characteristic of this model where there is an early phase of inflamed bowel and a late phase that is dominated by tissue fibrosis. By studying the MT in both phases, we demonstrated that MT is clearly sensitive to changes in fibrosis but is relatively insensitive to inflammation. As in the human disease, inflammation and fibrosis are closely linked and do not exist independently in the chronic phase of PG-PS–induced enterocolitis. Therefore, definitive proof of this concept will await histologic studies in humans. Our findings support our hypothesis and serve as a proof of concept that MT can noninvasively help differentiate fibrotic bowel from inflamed bowel in an animal model of Crohn disease.

Imaging with MT has the potential to be readily available for implementation in clinical practice. It uses a pulse sequence available on many MR imaging units currently in use in clinical practice. Implementation of this sequence does not require hardware upgrades but is a matter of software programming. We are currently conducting in vivo human MT imaging to study this technique, determine its resolution, and demonstrate its reliability and accuracy in patients with Crohn disease. If MT is found to be similarly sensitive to fibrosis in the human bowel wall, it may directly benefit patient care. Having the ability to quantify intestinal fibrosis should aid the clinician in determining if a patient with obstructive symptoms has a fibrotic stricture requiring surgery or dilation or if he or she has an inflammatory stricture that is more likely to respond to escalation of medical management.

Our study had the following limitations. First, the PG-PS model develops fibrosis in a segmental fashion, spreading out from the region of injection. Because the cecum in rats is large and mobile, the exact position of the cecum injected cannot be identified on imaging studies. This is a disadvantage as we may not be

measuring the ROI in the region of maximal fibrosis. However, this does improve our ability to be blinded to the treatment group when assessing the MR images. In addition, measuring the cecum circumferentially and averaging the ROIs across fibrotic and nonfibrotic regions would result in a lower mean MT ratio due to regression to the mean. Therefore, if the results of this study are affected by this, then our data would under-represent the strength of the association between MT ratio and fibrosis. The other limitation to this study, as in other studies of MR imaging of the intestines, is bowel motility. We performed MR imaging in sedated rats without the use of antimotility agents. Normal peristaltic motion creates substantial movement artifact, which interferes with image quality. In clinical practice, patients are frequently given an antimotility agent such as glucagon to decrease motion artifact. In this study, no antimotility agents were given. We did, however, exclude images that were of sufficiently poor quality to be uninterpretable. In imaging of other organs such as heart and lung, images can be gated for rhythmic movement. Future advances in programming may enable us to account for more complex motion such as peristalsis, making imaging of the bowel more practical.

In summary, we have demonstrated that MT can help detect fibrosis and that the MT ratio correlates with tissue collagen levels and is sensitive to changes in fibrosis over time.

Practical applications: A noninvasive method for determining the fibrotic content of small bowel strictures in Crohn disease could be used to inform treatment decisions. Prospective human studies will need to be performed to determine how this method alters patient outcomes. MT may also provide a tool to monitor changes in fibrosis over time and may lend insight into the natural history of Crohn disease. MT may also be useful to study the effect of current and nascent therapies on altering intestinal fibrosis.

References

1. Zimmermann EM, Lund PK. Fibrogenesis in inflammatory bowel disease. In: Kirsner J, ed. Inflammatory bowel disease. Philadelphia, Pa: Saunders, 2003.
2. Pucilowska JB, Williams KL, Lund PK. Fibrogenesis. IV. Fibrosis and inflammatory bowel disease: cellular mediators and animal models. Am J Physiol Gastrointest Liver Physiol 2000;279(4):G653–G659.
3. Kumagai S, Kawano S, Atsumi T, et al. Vertebral fracture and bone mineral density in women receiving high dose glucocorticoids for treatment of autoimmune diseases. J Rheumatol 2005;32(5):863–869. [Published correction appears in J Rheumatol 2005;32(7):1414.]
4. Bollet AJ, Black R, Bunim JJ. Major undesirable side-effects resulting from prednisolone and prednisone. J Am Med Assoc 1955; 158(6):459–463.
5. Whitworth JA. Adrenocorticotrophin and steroid-induced hypertension in humans. Kidney Int Suppl 1992;37:S34–S37.
6. Saag KG, Koehnke R, Caldwell JR, et al. Low dose long-term corticosteroid therapy in rheumatoid arthritis: an analysis of serious adverse events. Am J Med 1994;96(2):115–123.
7. Brenner DJ, Hall EJ. Computed tomography—an increasing source of radiation exposure. N Engl J Med 2007;357(22):2277–2284.
8. Yaffe BH, Korelitz BI. Prognosis for nonoperative management of small-bowel obstruction in Crohn's disease. J Clin Gastroenterol 1983;5(3):211–215.
9. Wolff SD, Eng J, Balaban RS. Magnetization transfer contrast: method for improving contrast in gradient-recalled-echo images. Radiology 1991;179(1):133–137.
10. Hashemi R, Bradley WG, Lisanti CJ. MRI: the basics. 2nd ed. Philadelphia, Pa: Lippincott Williams & Wilkins, 2004.
11. Zimmermann EM, Sartor RB, McCall RD, Pardo M, Bender D, Lund PK. Insulinlike growth factor I and interleukin 1 beta messenger RNA in a rat model of granulomatous enterocolitis and hepatitis. Gastroenterology 1993;105(2):399–409.
12. Grad J, Bryant RG. Nuclear magnetic cross-relaxation spectroscopy. J Magn Reson 1990; 90(1):1–8.
13. Henkelman RM, Huang X, Xiang QS, Stanisz GJ, Swanson SD, Bronskill MJ. Quantitative interpretation of magnetization transfer. Magn Reson Med 1993;29(6):759–766.
14. Ramani A, Dalton C, Miller DH, Tofts PS, Barker GJ. Precise estimate of fundamental in-vivo MT parameters in human brain in clinically feasible times. Magn Reson Imaging 2002;20(10):721–731.
15. Sartor RB, Cromartie WJ, Powell DW, Schwab JH. Granulomatous enterocolitis induced in rats by purified bacterial cell wall fragments. Gastroenterology 1985;89(3): 587–595.
16. Rath HC, Herfarth HH, Ikeda JS, et al. Normal luminal bacteria, especially *Bacteroides* species, mediate chronic colitis, gastritis, and arthritis in HLA-B27/human beta2 microglobulin transgenic rats. J Clin Invest 1996;98(4):945–953.
17. Herfarth HH, Böcker U, Janardhanam R, Sartor RB. Subtherapeutic corticosteroids potentiate the ability of interleukin 10 to prevent chronic inflammation in rats. Gastroenterology 1998;115(4):856–865.
18. McCall RD, Haskill S, Zimmermann EM, Lund PK, Thompson RC, Sartor RB. Tissue interleukin 1 and interleukin-1 receptor antagonist expression in enterocolitis in resistant and susceptible rats. Gastroenterology 1994;106(4):960–972.
19. International Commission on Illumination. Proceedings of the CIE Expert Symposium '97 on Colour Standards for Image Technology. Vienna, Austria: Commission Internationale de l'éclairage, CIE Central Bureau, 1998.
20. Schwartz MW, Cowan WB, Beatty JC. An experimental comparison of RGB, YIQ, LAB, HSV, and opponent color models. ACM Trans Graph 1987;6(2):123–158.
21. Jones B, Fishman EK, Hamilton SR, et al. Submucosal accumulation of fat in inflammatory bowel disease: CT/pathologic correlation. J Comput Assist Tomogr 1986;10(5): 759–763.
22. Bodily KD, Fletcher JG, Solem CA, et al. Crohn disease: mural attenuation and thickness at contrast-enhanced CT enterography—correlation with endoscopic and histologic findings of inflammation. Radiology 2006; 238(2):505–516.
23. Jacene HA, Ginsburg P, Kwon J, et al. Prediction of the need for surgical intervention in obstructive Crohn's disease by 18F-FDG PET/CT. J Nucl Med 2009;50(11):1751–1759.
24. Maconi G, Carsana L, Fociani P, et al. Small bowel stenosis in Crohn's disease: clinical, biochemical and ultrasonographic evaluation of histological features. Aliment Pharmacol Ther 2003;18(7):749–756.
25. Nylund K, Leh S, Immervoll H, et al. Crohn's disease: comparison of in vitro ultrasonographic images and histology. Scand J Gastroenterol 2008;43(6):719–726.
26. Kim K, Johnson LA, Jia C, et al. Noninvasive ultrasound elasticity imaging (UEI) of Crohn's disease: animal model. Ultrasound Med Biol 2008;34(6):902–912.
27. Messaris E, Chandolias N, Grand D, Pricolo V. Role of magnetic resonance enterography in the management of Crohn disease. Arch Surg 2010;145(5):471–475.
28. Punwani S, Rodriguez-Justo M, Bainbridge A, et al. Mural inflammation in Crohn disease: location-matched histologic validation of MR imaging features. Radiology 2009; 252(3):712–720.
29. Masselli G, Brizi GM, Parrella A, Minordi LM, Vecchioli A, Marano P. Crohn disease: magnetic resonance enteroclysis. Abdom Imaging 2004;29(3):326–334.
30. Lawrance IC, Welman CJ, Shipman P, Murray K. Correlation of MRI-determined small bowel Crohn's disease categories with medical response and surgical pathology. World J Gastroenterol 2009;15(27):3367–3375.